

Thermoelectric properties and microstructure of *c*-axis-oriented $\text{Ca}_3\text{Co}_4\text{O}_9$ thin films on glass substrates

Y. F. Hu

Materials Science Department, Brookhaven National Laboratory, Upton, New York 11973

E. Sutter

Center for Functional Nanomaterials, Brookhaven National Laboratory, Upton, New York 11973

W. D. Si

Physics Department, Brookhaven National Laboratory, Upton, New York 11973

Qiang Li^{a)}

Materials Science Department, Brookhaven National Laboratory, Upton, New York 11973

(Received 25 April 2005; accepted 30 August 2005; published online 19 October 2005)

c-axis-oriented $\text{Ca}_3\text{Co}_4\text{O}_9$ thin films have been grown directly on glass (fused silica) substrate by pulsed laser deposition. Detailed microstructure analysis showed stacking faults abundant throughout the films. However, the Seebeck coefficient ($\sim 130 \mu\text{V}/\text{K}$) and resistivity ($\sim 4.3 \text{ m}\Omega \text{ cm}$) of these films on glass substrate at room temperature were found comparable to those of the single-crystal samples. The presence of these structural defects could reduce thermal conductivity, and thus enhance the overall performance of cobaltate films to be potentially used in the thermoelectric devices. © 2005 American Institute of Physics. [DOI: 10.1063/1.2117615]

Recently, layered cobaltates have emerged as promising thermoelectric (TE) materials due to their excellent TE properties. Calcium cobaltate is among the best thermoelectric oxides, and thus has been extensively studied in single crystalline and bulk polycrystalline forms.¹⁻⁶ The studies of TE properties of cobaltate films are somewhat limited.⁷⁻¹⁰ In many TE applications, such as thermochemistry on a chip, biothermoelectric chip, and active cooling for microelectronic processor, film devices are required that allow localized cooling/heating at points of interest. High-quality TE thin films, having the crystal structure of single crystals, can have a low resistivity and a high Seebeck coefficient intrinsic to their electronic band structures. At the same time, thin films are expected to have thermal conductivity lower than that of the single crystals due to strong phonon scatterings at both surfaces and film/substrate interfaces.^{11,12} Hence, high-quality films could result in higher value of ZT . ZT is the figure of merit that measures the performance of a TE material, and is defined as $ZT = S^2 T / (\rho \kappa)$, where T , S , ρ , and κ are the absolute temperature, Seebeck coefficient, electrical resistivity, and thermal conductivity, respectively.

We have recently reported growth of high-quality *c*-axis-oriented $\text{Ca}_3\text{Co}_4\text{O}_9$ thin films directly on Si (100) wafers by pulsed laser deposition (PLD).¹³ Cross-sectional transmission electron microscopy (TEM) characterization revealed that the $\text{Ca}_3\text{Co}_4\text{O}_9$ film on a Si (100) substrate had a nearly perfect crystalline structure. The Seebeck coefficient and resistivity of the $\text{Ca}_3\text{Co}_4\text{O}_9$ thin films are $126 \mu\text{V}/\text{K}$ and $4.3 \text{ m}\Omega \text{ cm}$, respectively, at room temperature, comparable to those of the single-crystal samples. Thus, reducing the thermal conductivity seems to be an effective way to further enhance the TE performance of $\text{Ca}_3\text{Co}_4\text{O}_9$ films.

It is well known that suitable structural defects, such as stacking faults and grain boundaries, will create additional scattering mechanisms in the material and reduce the thermal

conductivity. This effect has been observed in both bulk and thin-film superlattice samples.^{14,15} However, the introduction of defects may also decrease the Seebeck coefficient and electrical conductivity. The ultimate goal is to engineer the structural defects in the films that block the phonon transport but not the charge carriers. Recently, we have prepared $\text{Ca}_3\text{Co}_4\text{O}_9$ films on various single crystalline, polycrystalline, and amorphous substrates under different conditions. In this letter, we report that the $\text{Ca}_3\text{Co}_4\text{O}_9$ films grown on a glass substrate (fused silica or amorphous SiO_2) have those desirable structural defects that may result in lower thermal conductivity. Remarkably, the Seebeck coefficient ($\sim 130 \mu\text{V}/\text{K}$) and resistivity ($\sim 4.3 \text{ m}\Omega \text{ cm}$) at room temperature are still comparable to those of the best single-crystal samples.

Our $\text{Ca}_3\text{Co}_4\text{O}_9$ thin films were grown *in situ* by the PLD process. A commercial glass (fused silica) wafer (from Sydor Optics, Inc.) was used as the substrate. The substrates were cleaned in acetone and methanol prior to the deposition. Films about 1600 \AA thick were deposited at a substrate temperature of $700 \text{ }^\circ\text{C}$ with a laser energy density of $\sim 1.5 \text{ J}/\text{cm}^2$, under an oxygen pressure of 300 mTorr. After deposition, the films were cooled to room temperature in $\sim 1 \text{ atm}$ of oxygen. Figure 1 shows the x-ray diffraction (XRD) patterns for the $\text{Ca}_3\text{Co}_4\text{O}_9$ film grown on the glass substrate. The XRD patterns exhibit nearly perfect *c*-axis alignment for the thin film. (Note: The log scale used for the intensity counts.) No diffraction peaks due to impurity phases were observed.

A cross-sectional TEM overview image of the $\text{Ca}_3\text{Co}_4\text{O}_9$ /glass interface region is shown in Fig. 2. Two interfaces can be seen in Fig. 2, indicated by Arrows 1 and 2. Between the crystalline $\text{Ca}_3\text{Co}_4\text{O}_9$ film and glass substrate, there is an amorphous layer $\sim 10 \text{ nm}$ thick, whose composition is related to that of $\text{Ca}_3\text{Co}_4\text{O}_9$. This is very similar to the $\text{Ca}_3\text{Co}_4\text{O}_9$ film grown on the Si(100) substrate, the native oxide of which was not removed prior to deposition, where

^{a)}Electronic mail: qiangli@bnl.gov

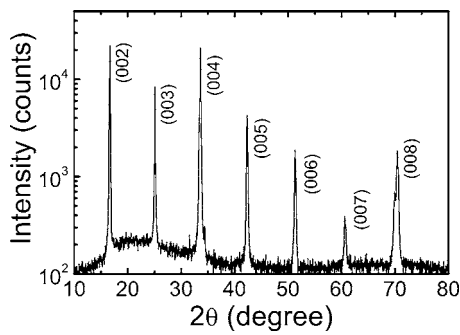


FIG. 1. XRD patterns for a 1600 Å thick $\text{Ca}_3\text{Co}_4\text{O}_9$ film grown on glass substrate.

the growth also starts amorphous before it turns to small grain crystalline and excellent quality crystalline throughout the film.¹³

High-resolution electron microscopy (HREM) images of the layered $\text{Ca}_3\text{Co}_4\text{O}_9$ film near the interface are shown in Fig. 3. Figure 3(a) shows well-ordered layer structures of $\text{Ca}_3\text{Co}_4\text{O}_9$ stacked along the c axis. These structures were observed near the interface and everywhere inside the $\text{Ca}_3\text{Co}_4\text{O}_9$ films. The structural defects in the films are mostly stacking faults, abundant throughout the films at various length scales. Sometimes, long stacking faults could be found across the entire TEM specimen. Nanosized second-phase materials (typically 5–10 nm) were also observed in certain regions close to the interface, but hardly present in the interior of the film. In Fig. 3(b)—showing a TEM image taken near the interface—Arrow 1 indicates a stacking fault that alters the periodic sequence of layers. Arrow 2 indicates a second phase, with a period of the layers that differs from the main phase of the film, possibly due to different composition ratios of Ca/Co. This was also observed by Yoshida *et al.*⁷ in the $\text{Ca}_3\text{Co}_4\text{O}_9$ film grown on $\text{SrTiO}_3(100)$ substrate.

Figure 4 shows the temperature dependence of the resistivity ρ and Seebeck coefficient S for a $\text{Ca}_3\text{Co}_4\text{O}_9$ film grown on glass substrate, together with the data of a $\text{Ca}_3\text{Co}_4\text{O}_9$ film grown on Si (100) substrate. The ρ - T curve of the film on glass exhibits very weak metallic behavior at $T > 170$ K, and shows a broad minimum with decreasing temperature. At low temperatures, the ρ - T curve exhibits a diverging behavior due to the magnetic phase transition of cobaltates. This temperature dependence is similar to that for the $\text{Ca}_3\text{Co}_4\text{O}_9$ single-crystal in-plane resistivity $\rho_{ab}(T)$ (Ref. 5) and the film on Si (100) substrate. However, the slope of the ρ - T curve at

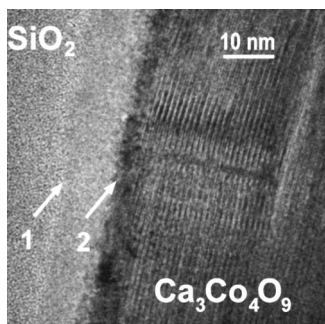


FIG. 2. The HREM overview image of the $\text{Ca}_3\text{Co}_4\text{O}_9$ /glass interface region for a $\text{Ca}_3\text{Co}_4\text{O}_9$ film. Between the glass substrate (indicated by Arrow 1) and well-ordered $\text{Ca}_3\text{Co}_4\text{O}_9$ layered film (indicated by Arrow 2), there is an amorphous region where the composition is related to that of $\text{Ca}_3\text{Co}_4\text{O}_9$.

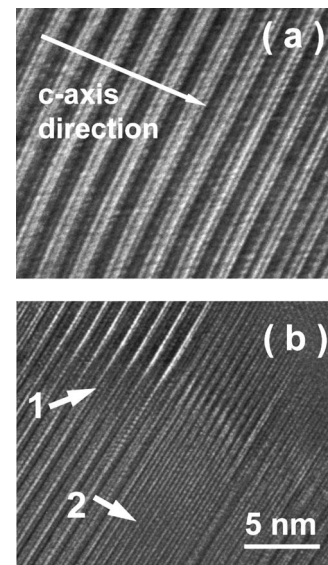


FIG. 3. (a) The HREM image of the $\text{Ca}_3\text{Co}_4\text{O}_9$ film grown on glass substrate, showing the layered $\text{Ca}_3\text{Co}_4\text{O}_9$ structure. (b) The HREM image of a $\text{Ca}_3\text{Co}_4\text{O}_9$ film region consisting of a stacking fault and a second phase material, indicated by Arrows 1 and 2, respectively.

the high-temperature region for films on Si (100) and single crystals are much steeper than the present films on glass, as is clearly shown in the inset to Fig. 4(a). The $\text{Ca}_3\text{Co}_4\text{O}_9$ film grown on the Si (100) substrate has almost perfect crystallinity and its ρ - T curve is close to that of the single-crystal samples.¹³ The $\text{Ca}_3\text{Co}_4\text{O}_9$ film grown on a glass substrate has a significant amount of stacking faults. It is not surprising that these defects cause additional carrier scattering, which changes the overall ρ - T behavior. This effect appears to be more pronounced at low temperature, but much less at a high temperature. At $T > 300$ K, the difference in the resistivity of films on glass and single-crystalline substrates are, in fact, very small. The mechanism for this is certainly worthy of further investigation, but is beyond the scope of this letter.

The Seebeck coefficient of the $\text{Ca}_3\text{Co}_4\text{O}_9$ films was measured using a four-terminal steady-state method in a Quantum Design PPMS system. Figure 4(b) shows the Seebeck

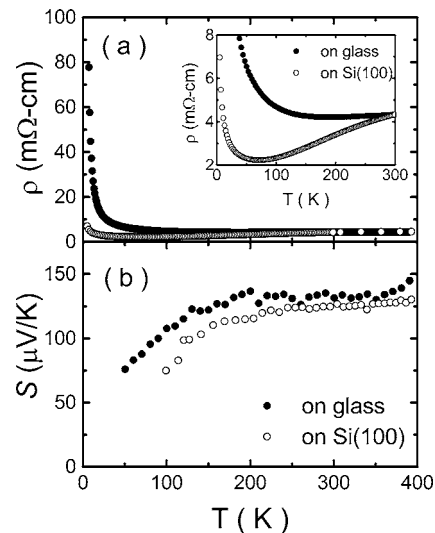


FIG. 4. The temperature dependence of the (a) resistivity and (b) thermoelectric power for $\text{Ca}_3\text{Co}_4\text{O}_9$ films on glass substrate (closed circle) and Si (100) substrate (open circle). An expanded view of (a) is shown as an inset.

coefficient S as a function of temperature for a $\text{Ca}_3\text{Co}_4\text{O}_9$ film on a glass substrate between 50 K and 400 K. S monotonically increases with temperature. At 300 K, the thermoelectric power for the $\text{Ca}_3\text{Co}_4\text{O}_9$ film on glass is around $130 \mu\text{V}/\text{K}$; very close to that of the single crystal sample⁶ and that of the film grown on Si (100) substrate.

Though there is no reliable method of directly measuring the *in-plane* thermal conductivity (κ) of thin films of a few hundred nm thickness, we expect that the $\text{Ca}_3\text{Co}_4\text{O}_9$ film on a glass substrate would have a substantially lower κ than that of the single-crystal samples. This is due to the strong phonon scattering at stacking faults, in addition to the scattering at film surfaces and film/substrate interfaces. Therefore, the ZT values of these films are expected to be better than the single-crystal samples. Furthermore, the glass substrate is an amorphous material and has very low thermal conductivity. Thus, cobaltate films on glass substrates will have additional advantages in practical TE device applications.

In summary, we demonstrate that *c*-axis-oriented thin films of $\text{Ca}_3\text{Co}_4\text{O}_9$ can be grown directly on a glass substrate by PLD. Detailed microstructural analysis revealed good overall *c*-axis alignment of the $\text{Ca}_3\text{Co}_4\text{O}_9$ film, with a high density of stacking faults throughout the films. The measured resistivity and Seebeck coefficient at temperatures above 300 K are similar to that found in the single-crystal samples. Devices utilizing $\text{Ca}_3\text{Co}_4\text{O}_9$ on amorphous SiO_2 should have enhanced thermoelectric performance due to a reduced overall thermal conductivity, caused by the stacking faults in

the films and by the intrinsically low substrate thermal conductivity.

This work was supported by the U.S. Dept. of Energy, Office of Basic Energy Science, under Contract No. DE-AC-02-98CH10886.

- ¹S. Li, R. Funahashi, I. Matsubara, K. Ueno, and H. Yamada, *J. Mater. Chem.* **9**, 1659 (1999).
- ²S. Li, R. Funahashi, I. Matsubara, K. Ueno, and H. Yamada, *J. Mater. Chem.* **12**, 2424 (2000).
- ³R. Funahashi, I. Matsubara, S. Sodeoka, H. Ikuta, T. Takeuchi, and U. Mizutani, *Jpn. J. Appl. Phys., Part 2* **39**, L1127 (2000).
- ⁴Y. Miyazaki, K. Kudo, M. Akoshima, Y. Ono, Y. Koike, and T. Kajitani, *Jpn. J. Appl. Phys., Part 2* **39**, L531 (2000).
- ⁵A. Masset, C. Michel, A. Maignan, M. Hervieu, O. Toulemonde, F. Studer, B. Raveau, and J. Hejtmanek, *Phys. Rev. B* **62**, 166 (2000).
- ⁶M. Shikano and R. Funahashi, *Appl. Phys. Lett.* **82**, 1851 (2003).
- ⁷Y. Yoshida, T. Kawai, Y. Takai, and M. Yamaguchi, *J. Ceram. Soc. Jpn.* **110**, 1080 (2002).
- ⁸I. Matsubara, R. Funahashi, and M. Shikano, *Appl. Phys. Lett.* **80**, 4729 (2002).
- ⁹H. Minami, K. Itaka, H. Kawaji, Q. J. Wang, H. Koinuma, and M. Lippmaa, *Appl. Surf. Sci.* **197**, 442 (2002).
- ¹⁰H. W. Eng, W. Prellier, S. Hebert, D. Grebille, L. Mechin, and B. Mercey, *J. Appl. Phys.* **97**, 013706 (2005).
- ¹¹L. D. Hicks and M. D. Dresselhaus, *Phys. Rev. B* **47**, 12727 (1993).
- ¹²R. Venkatasubramanian, E. Siivola, T. Colpitts, and B. O'Quinn, *Nature (London)* **413**, 597 (2001).
- ¹³Y. F. Hu, W. D. Si, E. Sutter, and Qiang Li, *Appl. Phys. Lett.* **86**, 082103 (2005).
- ¹⁴M. F. Crommie and A. Zettl, *Phys. Rev. B* **43**, 408 (1991).
- ¹⁵S.-M. Lee, D. G. Cahill, and R. Venkatasubramanian, *Appl. Phys. Lett.* **70**, 2957 (1997).